Frontiers in Heat and Mass Transfer (FHMT), 19, 22 (2022)
DOI: 10.5098/hmt.19.22

Global Digital Central
ISSN: 2151-8629

Frontiers in Heat and Mass Transfer

Available at www.ThermalFluidsCentral.org

PERFORMANCE ANALYSIS OF LONGITUDINAL FIN JET PLATE SOLAR AIR HEATER UNDER CROSS FLOW CONDITION

Rajen Kumar Nayak[a,*], Ravi Shankar Prasad[a,†], Ujjwal Kumar Nayak[a], Amit Kumar Gupta[b]

[a]*Department of Mechanical Engineering, B.I.T. Sindri, Dhanbad, Jharkhand, PIN 828123, India*
[b]*Department of Chemical Engineering, B.I.T. Sindri, Dhanbad, Jharkhand, PIN 828123, India*

ABSTRACT

The present experimental work has been carried out for a solar air heater under cross flow condition having inline hole jet plate between bottom plate and absorber plate with longitudinal fins underside the absorber surface. The performance of this inline hole jet plate solar air heater is compared with the performance of jet plate solar air heaters without longitudinal fins under cross and non-cross flow conditions for similar geometrical and operational parameters. Results are presented for mass flow rates of air, $\dot{m}_1 = 0.020$ - 0.070 kg/sec, $\dot{m}_2 = 0.018$ - 0.041 kg/sec, flow Reynolds number, $Re_{ja2} = 2000$ - 8000, jet hole diameter, $D = 6.0$ mm, number of jet hole, $N = 561$, depth of bottom and upper channel, $Z_1 = 7.0$ cm, $Z_2 = 7.0$ cm, total air depth, $Z = 14.0$ cm, pitch of the fins, $p = 5.0$ cm, total number of fins, $N_f = 20$, height of fins, $L_f = 12.0$ mm, thickness of fins, $\delta_f = 3.0$ mm and tilt angle, $\theta = 22.6^o$. The experiment is performed during the winter season at IIT (ISM) Dhanbad, Jharkhand, India between 09:00 AM – 03:00 PM on hourly basis. The present investigation shows that the jet plate with longitudinal fins is more efficient than cross and non-cross flow jet plate solar air heater. The mass flow rates of air $\dot{m}_1$ and $\dot{m}_2$ substantially influences the collector efficiency, heat transfer coefficient and Nusselt number. Based on the experimental data, the empirical correlations for Nusselt number, friction factor and fin effectiveness have been developed.

Keywords: *cross flow, jet plate, longitudinal fins, fin efficiency, fin effectiveness*

1. INTRODUCTION

Impinging air jets are commonly employed method for achieving the high heat transfer rates and used in many similar engineering applications such as space heating and process heating for crops drying, etc. In recent years, several modifications are carried out by Prasad and Saini (1988), Gupta *et al.* (1993), Thombre and Sukhatme (1995), Sahu and Bhagoria (2005), Irfan and Emre (2006), Jaurker *et al.* (2006), Karsli (2007), Romdhane (2007), Akpinar and Kocyigit (2010) to improve the performance of flat plate solar air heaters by providing the artificial roughness, obstacles, baffles in various shapes and sizes having different arrangements and longitudinal fins over and underside of the absorber plate resulting in enhancement of the heat transfer coefficient (McAdams, 1954) between the absorber plate and the air flow in the channel.

Perry (1954) studied the heat transfer by convection from a hot gas jet to a plane surface. Gupta and Garg (1967) performed the performance studies on four solar air heaters, two of them were corrugated type and the other two were of mesh type, each employing the ordinary black-painted surfaces as collector. The rating parameters like the plate efficiency factor, heat removal efficiency factor, overall heat loss coefficient and the effective absorption coefficient are also reported. Kercher and Tabakoff (1970) analyzed heat transfer by a square array of round air jets impinging perpendicular to a flat surface including the effect of spent air. Correlation of the heat transfer performance in a semi-enclosed environment is developed. The correlation presents the effects of the jet spent air flowing perpendicular to the jets, the effects of the jet diameter, jet spacing and jet-to-surface distance. Metzger *et al.* (1979) studied heat transfer characteristics for inline and staggered arrays of circular jets with cross flow of spent air on a surface parallel to the jet orifice plate. The mean Nusselt numbers and streamwise Nusselt number profiles are presented as a function of Reynolds number and geometric parameters.

Florschuetz *et al.* (1981) analyzed jet array impingement with cross flow and developed the correlation of streamwise resolved flow and heat transfer distributions. Garg *et al.* (1983) studied the effect of enhanced heat transfer area in the conventional type solar air heaters. This heat transfer area is increased by employing rectangular fins, or by vee-corrugating the absorber plate of a conventional solar air heater. The comparison was made and addition of rectangular fins is found to be more effective. Prasad and Saini (1988) studied the effect of artificial roughness on heat transfer and friction factor in a solar air heater. The effect of height and pitch of the roughness elements on the heat transfer rate and friction is analyzed. Garg *et al.* (1989) made performance studies on a finned type solar air heater both theoretically and experimentally. In the experimental setup, the fins are attached to the upper plate of the conventional duct type solar air heater. The dependence of efficiency on the fin density is also analyzed. Garg *et al.* (1990, 1991) made a theoretical analysis on a new finned type solar air heater. A mathematical model is developed by writing the energy balance equations at the various interfaces of the system. Numerical simulation on the theoretical model is performed to evaluate the effect of the number of rectangular fins, the length of the fins equal to the length of the plates, the depth of the air channel and the air flow rate on the thermal performance of the solar air heater. The performance of a duct type solar air heater with rectangular fins in the air flow passage between the absorber and the rear plate was evaluated. The mathematical model predicted that the

[*]Department of Mechanical Engineering, B.I.T. Sindri, Dhanbad, Jharkhand, PIN 828123, India
[†] *Corresponding author. Email: rsprasad.me@bitsindri.ac.in*

Global Digital Central
ISSN: 2151-8629

shallower duct depth with the increased number and length of the rectangular fins improve the thermal performance of the solar air heater. But it increased the pressure drop also, resulting in increased energy requirement of pump for pumping the air through the collector. Therefore, to account for this expended energy, a new term 'effective heat gain' is introduced and computed separately in the different cases for comparison. These results are compared with the results of a conventional solar air heater with the same depth of duct and length.

Chaudhury and Garg (1991) did analytical study on cross and non-cross flow inline hole jet plate solar air heater. The air temperature increment in non-cross flow jet plate over the parallel plate air heater is found as 9.5ºC and 15.5ºC for depth (Z), 5.0 cm and 10.0 cm respectively at fixed mass flow rates of air. Verma *et al.* (1991) made a detailed theoretical parametric analysis of a corrugated solar air heater with and without cover. The optimum flow channel depth for the maximum heat absorption at the lowest collector cost is obtained. The effect of collector parameters and operating conditions on the collector performance is analyzed. Gupta *et al.* (1993) made an experimental investigation for heat and fluid flow in rectangular solar air heater ducts having transverse rib roughness on absorber plates. Correlations are developed for a Nusselt number and friction factor in terms of geometrical parameters of roughness, duct cross section and the flow Reynolds number. Thombre and Sukhatme (1995) performed an experimental study for the fully developed turbulent flow heat transfer and friction factor characteristics of shrouded, rectangular cross-sectioned longitudinal fin arrays with uninterrupted fins subjected to a uniform heat flux boundary condition at the fin base.

Sahu and Bhagoria (2005) investigated the augmentation of heat transfer coefficient using 90º broken transverse ribs on absorber plate of solar air heater. The results are compared with the results of smooth ducts under identical flow and thermal boundary conditions. Irfan and Emre (2006) made an experimental investigation of solar air heater with free and fixed fins. Jaurker *et al.* (2006) analyzed heat transfer and friction characteristics of solar air heater duct using rib-grooved artificial roughness. It is found that the heat transfer coefficient for rib-grooved arrangement is higher than that for the transverse ribs, whereas the friction factor is only slightly higher for rib-grooved arrangement as compared to that of rectangular transverse ribs having the identical rib height and spacing. Correlations for Nusselt number and friction factor is presented. Kurtbas and Turgut (2006) made an experimental investigation of solar air heater with free and fixed fins. Solar air heater with free and fixed fins is compared to flat plate solar air heater in terms of efficiency and exergy loss ratio. Singh (2006) made the performance studies on continuous longitudinal fins solar air heater. Karsli (2007) made a performance analysis of new design of solar air collectors for drying applications. This paper compares the performance of four types of air heating flat plate solar collectors and the effectiveness of the collectors in the decreasing order are found as a finned collector with an angle of 75°, a finned collector with an angle of 70°, a collector with tubes and a base collector. Romdhane (2007) made a comparative study of the different air solar collectors with introduction of baffles to enhance the heat transfer. The best configuration of baffles extending the trajectory of the air flow as well as increasing the speed of the air within the collector and the heat transfer is determined. Belusko *et al.* (2008) analyzed the performance of jet impingement in unglazed solar air collector. The flow distribution of jets along the collector and hole spacing are the important factors influencing the thermal efficiency of an unglazed solar air collector. Aharwal *et al.* (2009) studied heat transfer and friction characteristics of solar air heater ducts having integral inclined discrete ribs on absorber plate. This experimental research work presents the heat transfer and friction characteristics of solar air heater ducts with integral repeated discrete square ribs on the absorber plate. The effect of geometrical parameters i.e., the gap width and gap position has been examined. On the basis of experimental data, the correlations for Nusselt number and friction factor are developed as the function of roughness parameters of inclined discrete square ribs and flow Reynolds number. Akpinar and Kocyigit (2010) made an experimental investigation of thermal performance of solar air heater having three different types of obstacles on absorber plates. One case without any obstacle is also considered for comparison. The efficiencies, the heat gain factors and heat loss coefficients for the collectors are compared between the different cases. The correlations are developed from the experimental data to determine the optimum case and the optimum value of efficiency. The collector with obstacle has significantly better thermal performance than that without the obstacles. Xing *et al.* (2010) carried out an experimental and numerical investigations on heat transfer characteristics for cross flow inline and staggered hole jet plate solar air heater. The experiments are performed in a perspex model using a transient liquid crystal method. Local jet temperatures are measured at several positions on the impingement plate to evaluate the heat transfer coefficient exactly. The effects of variation in different impingement patterns, jet-to-plate spacing, crossflow schemes and jet Reynolds number on the local Nusselt number and the related pressure loss is studied experimentally. The numerical investigation showed that the CFD codes can be used in the thermal design process of such configurations.

Chabane *et al.* (2013a) performed an experimental study of the collector efficiency of single pass of solar air heaters with and without using fins attached under the absorbing plate. A comparison between the results shows a significant enhancement in the thermal efficiency of solar air collector with the fins than that without fins. Chabane *et al.* (2013b) made a thermal efficiency analysis of a single-flow solar air heater with different mass flow rates on a smooth plate. This study analyzed the thermal efficiency of flat plate solar air heaters at the different air flow rates. Optimum values of air mass flow rates are found to maximize the performance of the solar collector. Chauhan and Thakur (2013) performed an experimental investigation to study heat transfer and friction factor characteristics using impinging jets in a solar air heater duct. The effect of the various flow and geometrical parameters, like the jet diameter, streamwise and spanwise pitch has been investigated. Based on the experimental data, empirical correlations on heat transfer and friction factor for impinging jet solar air heater is developed. Chabane *et al.* (2014) made an experimental study of heat transfer and thermal performance of solar air heater with longitudinal fins.

Nayak and Singh (2016) carried out an experimental investigation of the effects of flow and channel spacings between jet plate and absorber plate in cross flow staggered hole jet plate solar air heater. The correlations for Nusselt number and friction factor are developed based on the experimental data. The present study concludes that the thermal performance of non-conventional jet plate solar air heater is always higher than the conventional parallel plate solar air heater. Aboghrara *et al.* (2017) made a performance analysis of solar air heater with jet impingement on corrugated absorber plate through circular jets in a duct flow of solar air heater. The effect of mass flow rate of air and solar radiation on outlet air temperature and efficiency are analyzed. The results are compared with the results of conventional solar air heater with the flat plat absorber. Experimental results show that the flow jet impingement on corrugated plat absorber and mass flow rate of air substantially influences the heat transfer of solar air heaters. Hasan *et al.* (2017) made an experimental investigation of jet array nanofluids impingement on photovoltaic and thermal collectors. The effect of different nanoparticles (SiC, TiO_2 and SiO_2) with water as its base fluid on the electrical and thermal performances of a photovoltaic thermal collector equipped with jet impingement is investigated and compared. The SiC with water nanofluid system is found to have the highest electrical and thermal efficiency. Nadda *et al.* (2017) studied heat transfer and friction loss in an impingement jets solar air heater with multiple arc protrusion obstacles. The correlations are developed for Nusselt number and friction factor from the experimental results. Rajaseenivasan *et al.* (2017) made an experimental investigation on the performance of an impinging jet solar air heater. The air is supplied through an impinging jet pipe, which contains the nozzles to distribute

Global Digital Central
ISSN: 2151-8629

the air on the solar air heater. The air released from the jet strikes on the absorber plate creates the turbulent mixing in flow and increases the rate of heat transfer. The experimental results of impinging jet solar air heater are compared with the results of conventional solar air heater. The results are examined by varying the angle of attack (0°, 10°, 20°, 30°, 60° and 90°) and the nozzle diameter (3 mm, 5 mm and 7 mm) with the different air mass flow rates. The results shows that the highest performance is obtained with the 30° angle of attack and the lowest performance is recorded with the 0° angle of attack. The reduction in the jet diameter increases the pressure loss in the collector. Soni and Singh (2017) made an experimental analysis of geometrical parameters on the performance of an inline jet plate solar air heater. The effect of flow and geometrical parameters like jet diameter and hydraulic diameter has been investigated. Collector efficiency increases and temperature rise parameters decrease with the increase in the mass flow rate for all geometrical configurations. Correlations are developed for Nusselt number in terms of Reynolds number, jet diameter and hydraulic diameter. Vinod and Singh (2017) made a thermo-hydraulic performance analysis of jet plate solar air heater under cross flow condition. The effect of geometrical parameters like hole configuration on the jet plate i.e., inline and staggered holes, and operational parameter like velocity of air impinging out of the jet holes on to surface of the absorber plate on the performance of jet plate solar air heater is analyzed for different air mass flow rates. The mass flow rate of air is found to influence heat transfer in the jet plate solar air heater. The performance of cross flow solar air heater with the inline hole jet plate is found better than that with the staggered hole jet plate. Aboghrara *et al.* (2018) performed a parametric study on the thermal performance and optimal design elements of solar air heater enhanced with jet impingement on a corrugated absorber plate. Matheswaran *et al.* (2018) made an analytical investigation of solar air heater with jet impingement using energy and exergy analysis. Sivakumar *et al.* (2019) performed an experimental thermodynamic analysis of a forced convection solar air heater using absorber plate with pin-fins. Kumar *et al.* (2020) developed the new correlations for heat transfer and pressure loss due to internal conical ring obstacles in an impinging jet solar air heater passage. Singh *et al.* (2020) utilized the circular jet impingement to enhance thermal performance of solar air heater. Yadav and Saini (2020) made a numerical investigation on the performance of a solar air heater using jet impingement with absorber plate.

Farahani and Shadi (2021) optimized roughened solar air heaters with impingement jets using the economic, energetic and exergetic analysis. Hassan and AboElfadl (2021) made a heat transfer and performance analysis of solar air heater having new transverse finned absorber of lateral gaps and central holes. Kumar *et al.* (2021a) developed heat transfer and friction factor correlations for an impinging air jets solar thermal collector with arc ribs on an absorber plate. Kumar *et al.* (2021b) made a comprehensive review of performance analysis of solar thermal collector with and without fins. Maithani *et al.* (2021) made a thermo-hydraulic and exergy analysis of solar air heater with inclined impinging jets on absorber plate. In the present study, a technique is employed in which the main air supply pipe is connected to the perforated branch pipes to supply air at an inclined angle for the air jet delivery. Thus, the ambient cool air is provided to the entire absorber plate surface as well as the inclined cool air jet impinging on the heated absorber plate. It is found that inclining the air jet is enhances the heat transfer. Moshery *et al.* (2021) studied the thermal performance of jet impingement solar air heater with transverse ribs absorber plate. Pazarlioğlu *et al.* (2021) made a numerical analysis of the effect of impinging jet on cooling of solar air heater with longitudinal fins. It is observed that the Nusselt number and thermal efficiency enhances by adding impingement jets and increasing the Reynolds number. It is found that the convection heat transfer coefficient increases with the increase in the height of fins. Salman *et al.* (2021a) made an exergy analysis of solar heat collector with air jet impingement on dimple-shape-roughened absorber surface. The indented dimple-roughened jet impingement solar heat collector is comparatively economical and have thermal performance better than the conventional single pass solar heat collectors under the same operating conditions. But due to the presence of jet impingement and dimple roughness, it has more friction loss and more pumping power is required to achieve the appropriate air flow. Salman *et al.* (2021b) made an experimental analysis of single loop solar heat collector with jet impingement over indented dimples. Based on the experimental results, the correlations are developed for the Nusselt number and friction factor as a function of the indented dimpled roughness parameters. Shetty *et al.* (2021) performed a numerical analysis of a solar air heater with circular perforated absorber plate. The thermo-hydraulic performance due to the elimination of laminar viscous layer is studied, which otherwise existed in a conventional solar air heater. The thermo-hydraulic efficiency of the collector is found to be directly proportional to the increase in vent diameter. This study infers that the circular geometry and vented absorber plate causes the vortex formation, which results in increase in turbulence induced heat transfer.

Das *et al.* (2022) made a numerical analysis of a solar air heater with jet impingement and compared between the performance of jet designs. The jet impingement on the absorber plate causes turbulence mixing of air in contact with the plate, increasing the heat transfer coefficient. The thermo-hydraulic performance of a solar air heater with jet impingement through conical protruding jets and circular jets is compared using finite element method based COMSOL Multiphysics software. The main reasons of its improved performance is more elongated streamlines and higher turbulent kinetic energy with increased mass flow rate leading to a wide jet affected area inside the duct. Flilihi *et al.* (2022) presented a CFD modeling using Ansys Fluent software to study the effect of absorber design on convective heat transfer in a flat plate solar collector. Several simulations were carried out to determine the influencing parameters allowing better performances of the collector as well as a good homogeneity of the temperature at the exit of the channel. Nayak *et al.* (2022) presented an analytical study of thermal performance of a jet plate solar air heater with the longitudinal fins under the cross flow and non-cross flow conditions. Salman *et al.* (2022) utilized the jet impingement on protrusion or dimple of heated plate to improve the performance of double pass solar heat collector. The effect of geometrical parameters of jet impingement on indented protrusion absorber in double-pass solar heat collector is investigated. Yadav and Saini (2022) made a thermo-hydraulic CFD analysis using Ansys Fluent software of impinging jet solar air heater with different jet geometries. This numerical study shows the thermal behaviour of impinging jet solar air heater with five different jet geometries i.e., triangular, rectangular, square, hexagonal and circular jets. Heat transfer as the Nusselt number and pumping loss as the friction factor is analyzed and compared for all the geometries under identical operating conditions.

However, a critical search of literature survey shows that there a few literatures are available on jet plate with longitudinal fins solar air heater. So, the present aim is to investigate the flow and heat transfer behaviour in longitudinal fins inline hole jet plate solar air heater under cross flow condition. A comparative study has been carried out for the present work with inline hole jet plate solar air heater without fins under cross and non-cross flow conditions. The new correlations for Nusselt number, friction factor and effectiveness of fin fitted with the absorber plate have been developed.

2. DESCRIPTION OF EXPERIMENTAL SETUP

2.1 Description of Experimental Setup and Procedure

The photographic view of the experimental setup, inline hole jet plate, absorber plate with longitudinal fins and elemental section of absorber plate with longitudinal fins are shown in Figs. 1(a), 1(b), 1(c) and 1(d) respectively. Figure 2 shows the schematic cross-sectional view of air flow in channels of the air heater under cross and non-cross flow condition. The sectional views of the absorber surface with and without longitudinal fins are presented in Fig. 3.

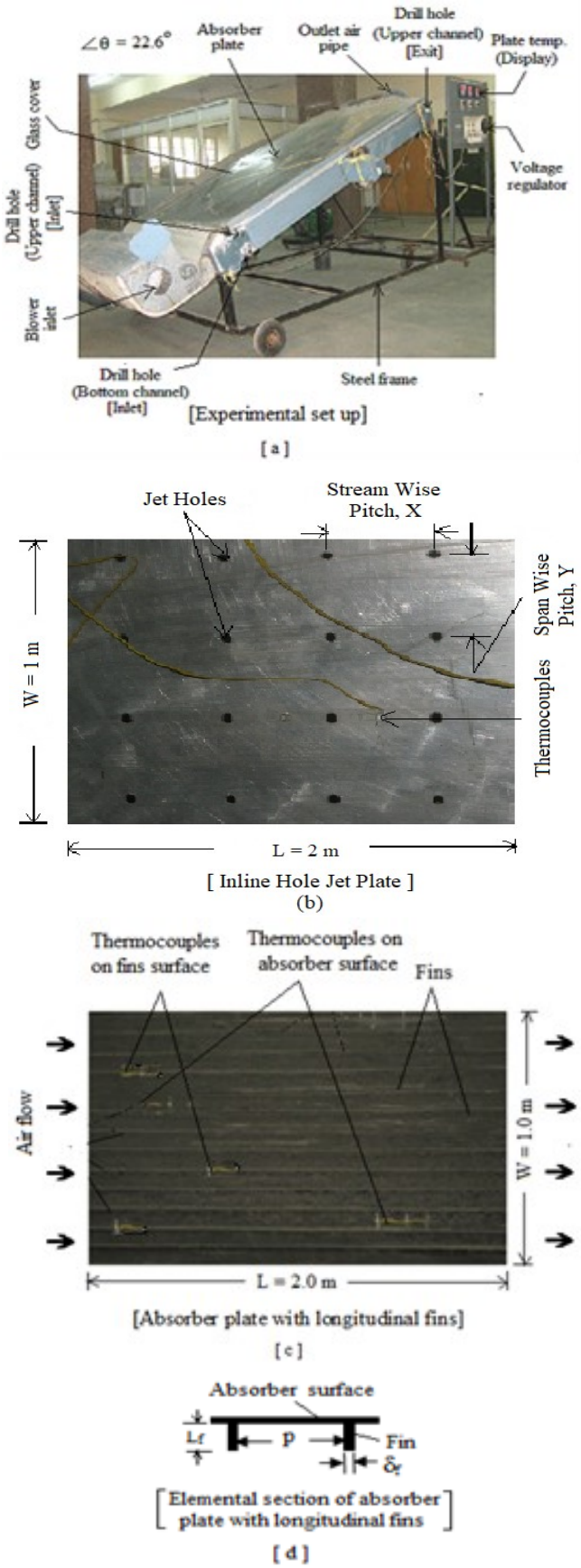

Fig. 1 Photographic view of (a) Experimental setup (b) Inline hole jet plate (c) Absorber plate with longitudinal fins and (d) Elemental section of absorber plate with longitudinal fins

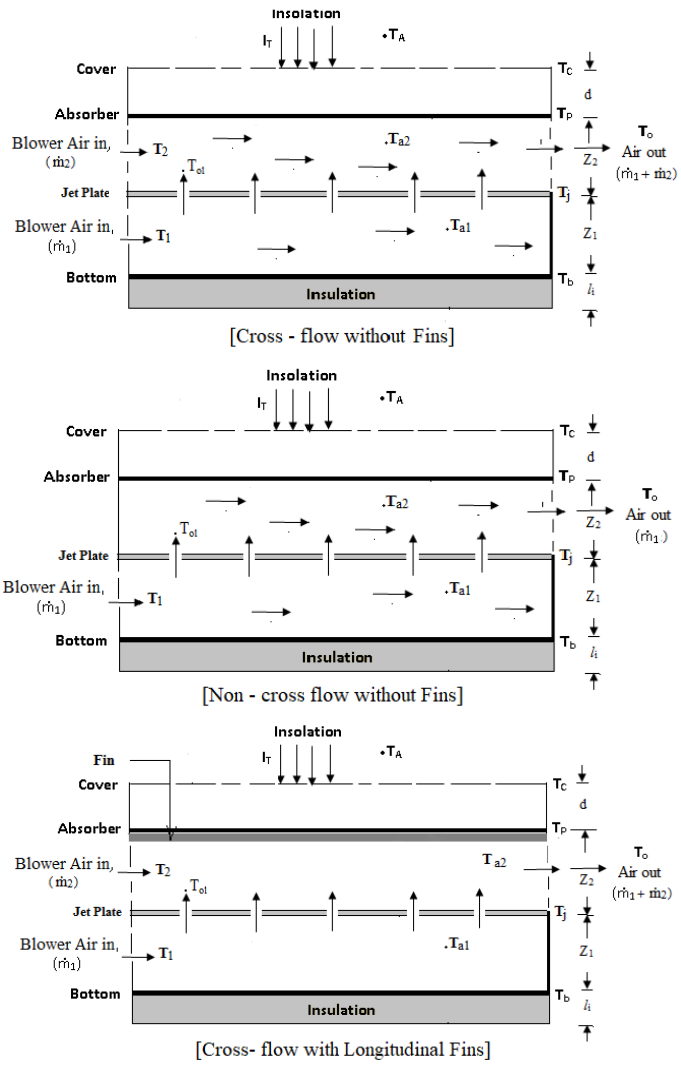

Fig. 2 Schematic cross-sectional view of air heaters with airflow in channels

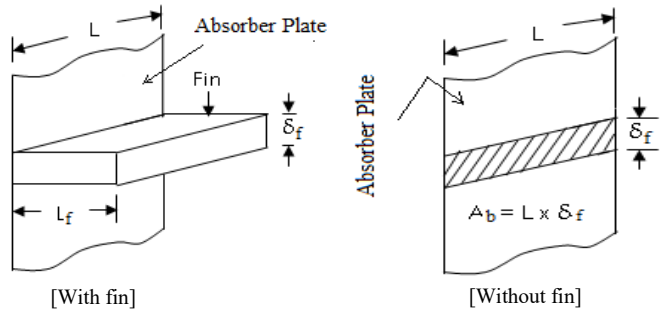

Fig. 3 Sectional view of absorber surface with and without fin for longitudinal fins jet plate solar air heaters

The M.S. plate of thickness 4 mm painted with black colour from inside to outside is used to make the frame of the solar air heater. For thermal insulation, the glass wool of 2.5 cm thickness (l_i) has been provided from the bottom and all the sides of the air heater. For each case of cross flow and non-cross flow conditions, the dimensions of black painted absorber plate made of mild steel, jet plate with inline hole made of aluminium alloy, toughened glass cover and frame of solar air heater are 2 m in length (L) and 1 m in width (W), the thicknesses of absorber plate, jet plate and toughened glass cover are 1 mm, 4 mm and 4 mm respectively. The total 561 numbers of the circular holes in jet plate (D = 6 mm), are arranged in inline manner. The total depth, Z between

Global Digital Central
ISSN: 2151-8629

absorber and bottom plate is 14.0 cm, which has been divided into two separate flow channels by inserting the jet plate between the absorber and bottom plate of the solar air heater. The depth of bottom channel (Z_1) and upper channel (Z_2) of cross and non-cross flow jet plate solar air heater is same i.e., 7.0 cm. There a total 20 longitudinal fins (L_f = 12 mm, δ_f = 3 mm, p = 5 cm) made of aluminium (k_{Al} = 237.0 W/mK) are attached underside of the absorber surface, which is shown in Fig. 1(c). For inserting the digital hot wire anemometer (DHWA), three drilled holes are provided for inlet air in bottom channel ($\dot{m}_1$), upper channel ($\dot{m}_2$), and one for exit of mixed air ($\dot{m}_1$ and $\dot{m}_2$) from the upper channel of the solar air heater. The whole structure is supported on a movable steel frame.

In operation, the inlet air at bottom channel, $\dot{m}_1$ and inlet air of upper channel, $\dot{m}_2$ of the air heater is supplied by a single blower regulated by a voltage regulator in case of cross flow condition. The mass flow rate of air $\dot{m}_1$ impinging out from the holes of jet plate only, because of closure of the exit channel, is mixed with $\dot{m}_2$ and exits from the upper channel in cross flow condition. In non-cross flow condition, inlet of the upper channel is closed so air $\dot{m}_1$ from the bottom channel passes through the jet holes and strikes the lower surface of the absorber plate and finally comes out from the upper channel exit. The inlet velocity $\overline{V_1}$ of air $\dot{m}_1$ and $\overline{V_2}$ of air $\dot{m}_2$ in bottom and upper channel respectively, outlet velocity, $\overline{V_o}$ of mixed air $\dot{m}_1$ and $\dot{m}_2$ in upper channel are measured by digital hot wire anemometer (DHWA).

2.2 Specifications of the Setup

The same instrument is used as mentioned in the previous section, for measuring the inlet temperature, T_1 of air $\dot{m}_1$ and T_2 of air $\dot{m}_2$, outlet temperature, T_o of mixed air $\dot{m}_1$ and $\dot{m}_2$ and ambient temperature, T_A in cross flow condition. The same method has been applied for measuring the inlet velocity, $\overline{V_1}$ and outlet velocity, $\overline{V_o}$ of air $\dot{m}_1$, inlet temperature, T_I and outlet temperature, T_o of air $\dot{m}_1$ in non-cross flow condition.

Table 1 Specification of the Setup

Nomenclature	*Specifications*
Length of solar air heater	L = 2 m
Width of collector	W = 1 m
Spacing between bottom and jet plate	Z_1 = 70 mm
Spacing between jet and absorber plate	Z_2 = 70 mm
Diameter of inline jet hole	D = 6 mm
Total number of jet holes	N = 561
Thickness of absorber plate	t = 1 mm
Thickness of jet plate	t = 4 mm
Thickness of toughened glass cover	t = 4.0 mm
Thickness of glass wool insulation	l_i = 2.5 cm
Width of the fins	W = 1 m
Length of the fins	L_f = 12 mm
Thickness of the fins	δ_f = 3 mm
Total number of longitudinal fins	N_f = 20
Tilt angle	θ = 22.6°

The accuracy of the instrument, DHWA is ± 0.05 m/s (velocity) and ± 0.8°C (temperature) with range of operating temperature 0°C to 50°C. The temperatures of absorber plate (T_P), jet plate (T_j) and bottom plate (T_b) are measured by the thermocouples having accuracy ± 2.2°C or 0.4% and range of operating temperature is 0°C to 1250°C. A total of ten thermocouples are embedded on lower and upper surface of the absorber plate and jet plate each. However, the total three and five numbers of thermocouple are embedded at bottom plate and attached fins on the absorber surface respectively. During the experiments, the solar intensity (I_T) has been recorded by using a pyranometer coupled with a digital millivoltmeter of accuracy ± 1% under clear sky condition. The tilt angle, θ of the solar air heater is given 22.6° with respect to the horizontal surface. The present experimental works have been carried out in the winter season with the clear sky at IIT (ISM) Dhanbad, Jharkhand, India. The air blower has been started for 45 minutes prior to the period in which data are taken and all test readings have been recorded between 09:00AM to 03:00 PM on hourly basis.

Table 2 Instruments used with their accuracy and ranges

Sl. No.	*Name of the instruments*	*Accuracy and Ranges*
1.	Digital Hot Wire Anemometer	± 0.05 m/s (in velocity) ± 0.8°C (in temperature) Range: 0°C to 50°C
2.	Pyranometer integrated with Digital millivoltmeter	± less than 1.0% (Under clear sky condition) Range: 0 to 10.0 mV with calibration constant = 129.31 W/m^2/mV
3.	Thermocouples	± 2.2°C or 0.4% Range: 0°C to 1250°C

3. DATA REDUCTION

For finding the thermal performance of the jet plate solar air heater under cross flow condition, the primary measurements taken are ambient temperature (T_A), solar intensity (I_T), inlet temperatures of air T_1 and T_2 at bottom and upper channels, outlet air temperature (T_o) and mass flow rates of air $\dot{m}_1$ and $\dot{m}_2$ in bottom and upper channel of the collector respectively. Each set of the experimental measurements consists of temperatures T_P at ten points, T_j at ten points and T_b at three points of the heated absorber plate, jet plate and bottom plate respectively. The experimental data has been obtained under steady state conditions and the operating range of the flow Reynolds number has been taken from 2500 to 8000. The above measurements have been used in the following equations to evaluate the thermal performance of jet plate solar air heater under cross flow condition. The convection heat transfer coefficient of absorber plate to jet air (h_{Pj}) has been expressed as,

$$h_{Pj} = \frac{(\dot{m}_1+\dot{m}_2)Cp(T_O-T_i)}{A(T_P-T_{a2})} \quad (1)$$

where $T_i = \frac{(\dot{m}_1T_1+\dot{m}_2T_2)}{(\dot{m}_1+\dot{m}_2)}$ is the inlet air temperature above jet plate in mixing of two flows of air $\dot{m}_1$ and $\dot{m}_2$ and

$T_{a2} = \frac{(\dot{m}_1T_1+\dot{m}_2T_2)+(\dot{m}_1+\dot{m}_2)T_O}{2(\dot{m}_1+\dot{m}_2)}$ is the air temperature at upper channel.

The collector efficiency (η_c) can be calculated as Gupta *et al.* (1993).

$$\eta_c = \frac{(\dot{m}_1+\dot{m}_2)C_p(T_O-T_A)}{I_TA} \quad (2)$$

The behaviour of collector efficiency (η_c) with respect to mass flow rates of air ($\dot{m}_1$ and $\dot{m}_2$) is shown in Fig. 5.

Flow Reynolds number, Re_{ja2} in the upper channel of the air heater is defined on the basis of its hydraulic diameter, D_2.

$$Re_{ja2} = \frac{\rho\overline{V}D_2}{\mu} \quad (3)$$

Here hydraulic diameter, D_2 and average velocity, $\overline{V}$ of the air in the upper channel can be calculated as,

D_2 = [4 x channel flow area / wetted surface] = $\frac{4WZ_2}{2(W+Z_2)}$ and $\overline{V} = \frac{(V_{aV}+\overline{V}_O)}{2}$ respectively.

The outlet velocity of air, $\overline{V}_o$ is taken on the basis of total mass flow rates of air ($\dot{m}_1$ + $\dot{m}_2$) in the upper channel of the air heater, whereas $\overline{V}_{aV}$ is the average velocity of jet air (V_j) and inlet velocity ($\overline{V}_2$) of air in upper channel of the air heater and it is expressed as,

$$\overline{V}_{aV} = \frac{(A_jV_j + A_2\overline{V}_2)}{(A_2 + A_j)}$$

In the above expression, jet air velocity, V_j has been calculated on the basis of mass flow rate of air, $\dot{m}_1$ in the bottom channel of the air heater.

Global Digital Central
ISSN: 2151-8629

Nusselt number, Nu_{Pj} in upper channel of the air heater has been expressed in terms of convection heat transfer coefficient, h_{Pj} (Chaudhury and Garg, 1991) and hydraulic diameter of the upper channel, D_2. Hence,

$$Nu_{Pj} = \frac{h_{Pj}D_2}{k_a} = F_1F_2(Re_D)^m \left(\frac{Z_2}{D}\right)^{0.091} \quad (4)$$

The Blassius equation has been used in the following equation to evaluate friction factor, f_s in the upper channel of the air heater.

$$f_s = 0.085(Re_{ja2})^{-0.25} \quad (5)$$

The variation of friction factor, f_s with Reynolds number, Re_{ja2} is shown in Fig. 7. Under steady state condition, the same method is applied for jet plate with longitudinal fins and non-cross flow jet plate solar air heater in primary measurements of T_A, I_T, T_1, T_2, T_o, $\dot{m}_1$, $\dot{m}_2$,, T_P, T_j and T_b. The same equations from (1) to (5) are used for jet plate solar air heater for inline hole under cross flow with longitudinal fins and jet plate solar air heater for inline hole under non-cross flow without longitudinal fins. Here only the hydraulic diameter (D_2) is replaced by equivalent hydraulic diameter (Sukhatme, 1996), $D_e = 4[pZ_2 - L_f\delta_f] / 2[(p + L_f]$ in Eq. (3) for jet plate with longitudinal fins solar air heater under cross flow condition and $\dot{m}_2$ has been considered as zero, i.e., $\dot{m}_2 = 0$ in non-cross flow condition. The fin efficiency (η_f) and fin effectiveness (ξ) of the rectangular fin are expressed as,

η_f = [(Actual heat transfer rate from the fins) / (Ideal heat transfer rate from the fin, if the entire fins are at base temperature)]

$$\eta_f = \left(\frac{Q_f}{Q_{mf}}\right) = \left[\frac{\left(h_{Pj}P_fk_{Al}A_C\right)^{1/2}(T_P - T_{a2})}{h_{Pj}A_f(T_P - T_{a2})}\right]$$

$$or, \eta_f = \left(\frac{Q_f}{Q_{mf}}\right) = \left[\frac{tanh(m'L_C)}{(m'L_C)}\right] \quad (6)$$

where, $m'L_C = L_C\left[\frac{2h_{Pj}}{(k_{Al}\delta_f)}\right]^{1/2}$

and $L_c = L_f + \delta_f/2$

The effectiveness of the fin,

$$\xi = \left(\frac{Q_f}{Q_{Nf}}\right) = \left[\frac{\left(h_{Pj}P_fk_{Al}A_C\right)^{1/2}(T_P - T_{a2})}{h_{Pj}A_b(T_P - T_{a2})}\right]$$

$$or, \xi = \left[\frac{k_{Al}P_f}{h_{Pj}A_b}\right]^{1/2} \quad (7)$$

where $P_f = (2L_f + \delta_f)$ and $A_b = L \times \delta_f$

4. UNCERTAINITY ANALYSIS

The errors associated due to experimental measurements are discussed in the previous section 2. For finding the fractional uncertainties in experimental results as suggested by Moffat (1988), the Kline and Klintock (1953) method has been used. Since, the uncertainties of heat transfer coefficient, h_{Pj}, collector efficiency, η_c and flow Reynolds number, Re_{ja2} are mainly related with ($\dot{m}_1$, $\dot{m}_2$, T_o, T_i, T_P, T_{a2}), ($\dot{m}_1$, $\dot{m}_2$, T_A, T_o, I_T) and (ρ, V_j, $\overline{V_2}$, $\overline{V_o}$) respectively. However, $\dot{m}_1$ is related with the density, ρ of air and $\overline{V_1}$. Similarly, $\dot{m}_2$ is related with density, ρ of air and $\overline{V_2}$ and density, ρ with temperature, T_A. Hence, finally the fractional uncertainties of h_{Pj}, η_c and Re_{ja2} are related with (T_A, $\overline{V_1}$, $\overline{V_2}$, T_o, T_i, T_P, T_{a2}), (T_A, $\overline{V_1}$, $\overline{V_2}$, T_o, I_T) and (T_A, V_j, $\overline{V_2}$, $\overline{V_o}$) respectively. Therefore, the fractional uncertainties of h_{Pj}, η_c and Re_{ja2} are found by the following equations:

$$\frac{\omega_{h_{Pj}}}{h_{Pj}} = \left[\left(\frac{\omega_{T_A}}{T_A}\right)^2 + \left(\frac{\omega_{\overline{V_1}}}{\overline{V_1}}\right)^2 + \left(\frac{\omega_{\overline{V_2}}}{\overline{V_2}}\right)^2 + \left(\frac{\omega_{\Delta T_1}}{\Delta T_1}\right)^2 + \left(\frac{\omega_{\Delta T_2}}{\Delta T_2}\right)^2\right]^{1/2} \quad (8)$$

where, $\Delta T_1 = (T_o - T_i)$ and $\Delta T_2 = (T_P - T_{a2})$

$$\frac{\omega_{\eta_c}}{\eta_c} = \left[\left(\frac{\omega_{T_A}}{T_A}\right)^2 + \left(\frac{\omega_{\overline{V_1}}}{\overline{V_1}}\right)^2 + \left(\frac{\omega_{\overline{V_2}}}{\overline{V_2}}\right)^2 + \left(\frac{\omega_{To}}{T_o}\right)^2 + \left(\frac{\omega_{I_T}}{I_T}\right)^2\right]^{1/2} \quad (9)$$

$$\frac{\omega_{Re_{ja2}}}{Re_{ja2}} = \left[\left(\frac{\omega_{T_A}}{T_A}\right)^2 + \left(\frac{\omega_{V_j}}{V_j}\right)^2 + \left(\frac{\omega_{\overline{V_2}}}{\overline{V_2}}\right)^2 + \left(\frac{\omega_{Vo}}{V_o}\right)^2\right]^{1/2} \quad (10)$$

The experiments are carried out in cross flow jet plate solar air heater with and without longitudinal fins attached underside the absorber surface and non-cross jet plate solar air heater for fixed jet hole diameter D (6.0 mm). The mean values and uncertainties of the variables h_{Pj}, η_c, Re_{ja2}, T_A, ΔT_1, ΔT_2, T_o, $\overline{V_1}$, $\overline{V_2}$, V_j, $\overline{V_o}$, and I_T are obtained and tabulated in Table 3.

Table 3 Uncertainty in the variables used

Sl. No.	*Variables*	*Mean value of the variables*	*Uncertainty*
1.	h_{Pj},	12.14 W/m^{2}K	0.006
2.	η_c,	38.24%,	0.005
3.	Re_{ja2},	4928.02	0.002
4.	T_A	26.04ºC	0.0001
5.	ΔT_1	4.73ºC	0.005
6.	ΔT_2	13.6ºC	0.004
7.	T_o	32.9ºC	0.001
8.	$\overline{V_1}$	0.63 m/s	0.002
9.	$\overline{V_2}$	0.36 m/s	0.005
10.	V_j	2.76 m/s	0.002
11.	$\overline{V_o}$	0.81 m/s	0.006
12.	I_T	621.2 W/m^2	0.003

5. RESULTS AND DISCUSSION

5.1 Variation of outlet air temperature (*To*) and collector efficiency (*ηc*) with mass flow rate for fixed jet hole diameter (*D*)

Figures 4 and 5 show the effect of mass flow rates of air on outlet air temperature (T_o) and collector efficiency (η_c) respectively, in inline hole jet plate solar air heater under cross flow condition with and without fins attached underside the absorber surface and inline hole jet plate solar air heater for fixed jet hole diameter, D (6 mm) under non-cross flow condition. For each air heater, the outlet air temperature (T_o) decreases and the collector efficiency (η_c) increases with increase in mass flow rate of air $\dot{m}_1$. Both T_o and η_c are found substantially higher in longitudinal fin jet plate solar air heater under cross flow condition as compared to jet plate solar air heater under cross and non-cross flow conditions. The increment in outlet air temperature, T_o in longitudinal fins jet plate solar air heater is due to addition of fins, which transfer more heat from the absorber surface to the moving air in the channel. The higher amount of heat transfer from the absorber surface enhances heat transfer coefficient (h_{Pj}) and collector efficiency (η_c) in this solar air heater for all the mass flow rates of air $\dot{m}_1$ and $\dot{m}_2$.

Similarly, the outlet air temperature in jet plate solar air heater under non-cross flow condition is found higher than the jet plate solar air heater under cross flow condition for mass flow rate of air $\dot{m}_1$ due to higher value of cross flow degradation factor, $F_2 = 1$ (Chaudhury and Garg, 1991). Since, the jet air velocity (V_j) increases with decrease in cross flow air, $\dot{m}_2$ through the upper channel for fixed mass flow rate of air, $\dot{m}_1$ and depth of upper channel ($Z_2 = 7.0$ cm). In case of non-cross flow condition of air ($\dot{m}_2 = 0$, $F_2 = 1$), the high jet air velocity (V_j) strikes the lower surface of the absorber plate and breaks the thermal boundary layer of the surface resulting in increase of outlet air temperature (T_o) and heat transfer coefficient (h_{Pj}), which enhances the collector efficiency (η_c). However, the collector efficiency (η_c) is lower in non-cross flow jet plate than cross flow jet plate solar air heater due to non-mixing of two flows of air $\dot{m}_1$ and $\dot{m}_2$. For $\dot{m}_1 = 0.04$ kg/s, the outlet air temperature (T_o) and collector efficiency (η_c) in longitudinal fin jet plate solar air heater are found 2.7ºC and 8.5% higher than cross flow jet plate solar air heater, whereas the gain in outlet air temperature (T_o) and collector efficiency (η_c) are found as 1.6ºC and 15% higher in longitudinal fin jet plate solar air heater than non-cross flow jet plate solar air heater respectively. Further, the maximum increment in outlet temperature (T_o) and collector

Global Digital Central
ISSN: 2151-8629

efficiency (η_c) in longitudinal fin jet plate solar air heater are found 8% and 15.2% higher than cross flow inline hole jet plate solar air heater respectively. However, the maximum increment in outlet temperature (T_o) and collector efficiency (η_c) in jet plate with longitudinal fins are 4.1% and 56.0% higher than non-cross jet plate solar air heater respectively.

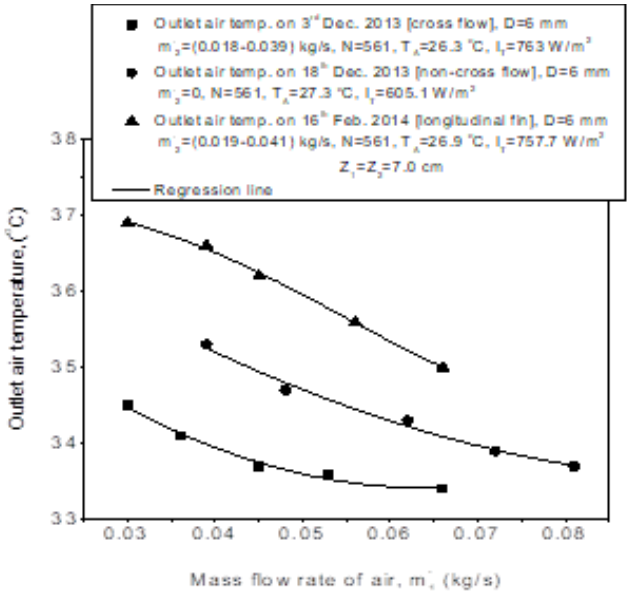

Fig. 4 Variation of outlet air temperature with mass flow rates of air in cross flow jet plate solar air heater with and without longitudinal fins attached underside the absorber surface and non-cross flow inline hole jet plate solar air heater at fixed jet hole diameter

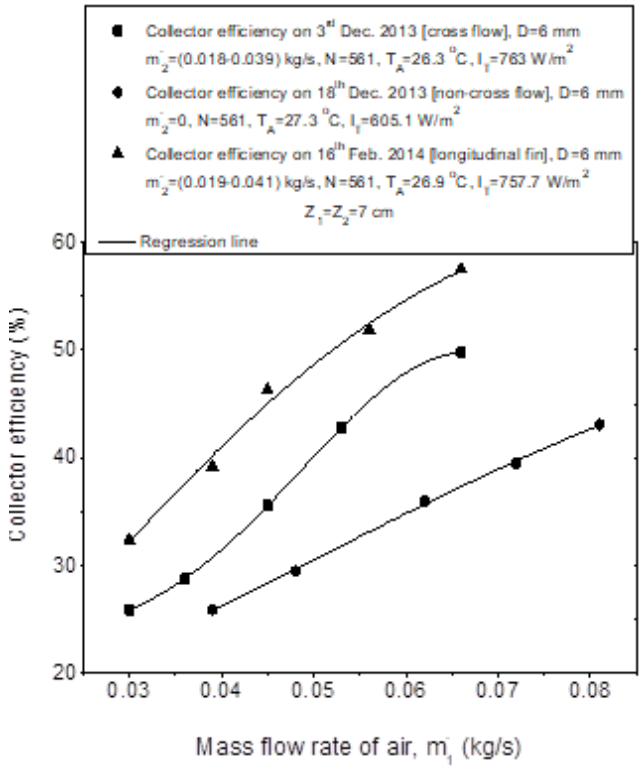

Fig. 5 Variation of collector efficiency with mass flow rate of air in cross flow jet plate solar air heater with and without fins attached underside the absorber surface and non-cross flow inline hole jet plate solar air heater at fixed jet hole diameter

5.2 Variation of Nusselt number (Nu_{Pj}) with flow Reynolds number (Re_{ja2}) at fixed jet hole diameter (D)

Figure 6 presents the variation of Nusselt number (Nu_{Pj}) with Reynolds number (Re_{ja2}) in jet plate solar air heater under cross flow condition with and without fins attached underside the absorber surface and non-cross flow jet plate solar air heater for fixed jet hole diameter (D = 6.0 mm). For the given range of the Reynolds number (Re_{ja2}), the Nusselt number (Nu_{Pj}) is found substantially higher in jet plate with longitudinal fins solar air heater than cross and non-cross flow jet plate solar air heater at fixed mass flow rate of air $\dot{m}_1$. Under similar geometrical configuration, the flow Reynolds number (Re_{ja2}) is a strong function of heat transfer enhancement, which validates the mass flow rate of air has significant effects on heat transfer in longitudinal fins jet plate solar air heater compared to cross and non-cross jet plate solar air heater. The reason behind enhanced heat transfer is attributed to the swirl motion generated due to the addition of fins underside of the absorber surface in the upper channel. This increases the turbulence, which leads to higher convection heat transfer coefficient(h_{Pj}) and Nusselt number (Nu_{Pj} in the longitudinal fin jet plate solar air heater. This also complies the Eq. (4) in which Nusselt number is directly associated with h_{Pj}. Further, the Nusselt number (Nu_{Pj}) is lower in non-cross flow jet plate than cross flow jet plate solar air heater for fixed mass flow rate of air $\dot{m}_1$ due non-availability of air, $\dot{m}_2$. Maximum increment in Nusselt number (Nu_{Pj}) is found as 53.6% and 57.1% higher in jet plate solar air heater with longitudinal fins with respect to cross and non-cross flow jet plate solar air heater respectively for fixed Reynolds number (Re_{ja2}).

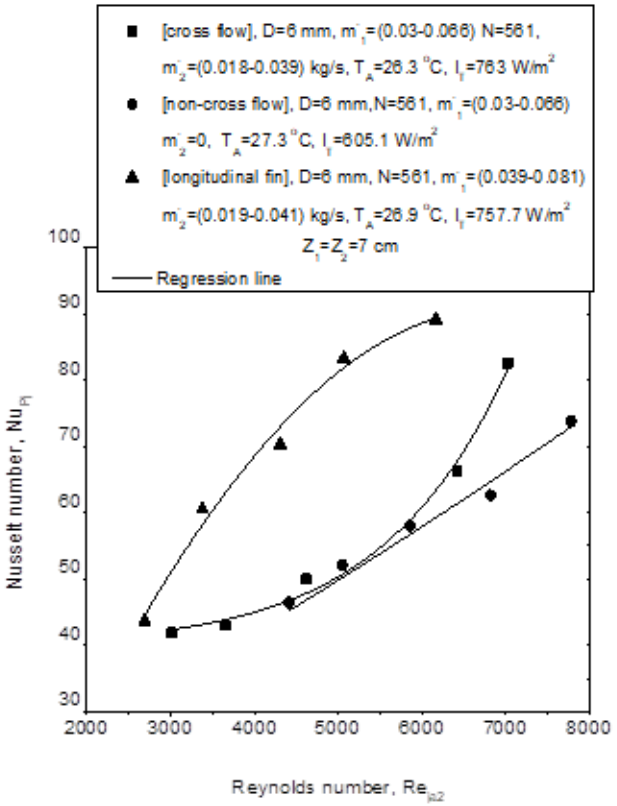

Fig. 6 Variation of Nusselt number with Reynolds number in cross flow jet plate air heater with and without fins attached underside the absorber surface and non-cross flow jet plate solar air heater for fixed jet hole diameter

5.3 Variation of friction factor (f_s) with Reynolds number (Re_{ja2}) at fixed jet hole diameter

At fixed jet hole diameter (D = 6 mm), the variation of friction factor (f_s) with Reynolds number (Re_{ja2}) in cross flow jet plate solar air heater with

and without fins attached underside the absorber surface and non-cross flow jet plate solar air heater is shown in Fig. 7. In each case of solar air heaters, it has been observed that the friction factor (f_s) decreases with increase of Reynolds number (Re_{ja2}). For all range of Reynolds number, the friction factor is found marginally higher in longitudinal fin jet plate solar air heater under cross flow condition as compared to jet plate solar air heater under cross flow condition due to the lower value of hydraulic diameter (D_e) of the upper flow channel. The pressure drop in the jet plate with longitudinal fins solar air heater is marginally higher in comparison to the cross flow jet plate solar air heater. So, for the same thermal performance, the pumping power required in jet plate solar air heater with longitudinal fins is more or less same as cross flow jet plate solar air heater.

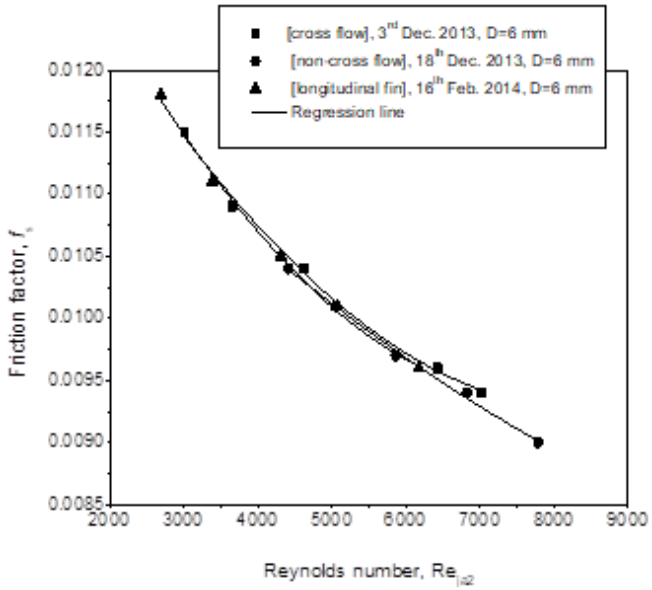

Fig. 7 Variation of friction factor with Reynolds number for cross flow jet plate solar air heater with and without fins are attached underside the absorber surface and non-cross flow jet plate solar air heater

5.4 Variation of fin efficiency (η_f) and the effectiveness of fin (ξ) of jet plate solar air heater with mass flow rate of air ($\dot{m}_1$) for fixed pitch of the fins (p)

Figure 8 shows that the variations of the fin efficiency (η_f) and effectiveness of the fin (ξ) with mass flow rates of air $\dot{m}_1$ and $\dot{m}_2$ in longitudinal fin jet plate solar air heater. It is observed that the fin efficiency (η_f) and effectiveness of the fin (ξ) decrease with increase in mass flow rates of air $\dot{m}_1$ and $\dot{m}_2$ for fixed jet hole diameter (D = 6 mm). For all range of the fin efficiency (η_f), the value of effectiveness of the fin (ξ) has been found greater than 1 (i.e., $\xi > 1$)indicating the importance of attaching the fins with the absorber plate.

5.5 Development of correlations for Nusselt number, friction factor and the effectiveness of fin in cross flow inline hole jet plate solar air heater with longitudinal fins

5.5.1 Correlation for Nusselt number

In the present study, the range of parameters for correlations are considered as $2515 \le Re_{ja2} \le 8000$, $0 \le Z_2 \le 0.07$. Based on the large set of experimental data, the Nusselt number has been correlated as,

$$Nu_{Pj} = 0.0035\ (Re_{ja2})^{0.8098}\ (Z_2 / p)^{8.5823} \quad (11)$$

From the above developed correlation, it is seen that the Reynolds number (Re_{ja2}) and depth of upper channel (Z_2) directly affect the Nusselt number due to the parameters Re_{ja2} and Z_2/p having positive exponent. The positive exponents show the dominancy of the terms Re_{ja2} and Z_2/p on heat transfer coefficient for fixed pitch of the fins (p). However, pitch of the fins (p) adversely affects the Nusselt number as the term, p having the negative exponent at fixed Z_2. The correlation coefficient of 0.92 indicates the goodness of fit in cross flow jet plate solar air heater with longitudinal fins as shown in Fig. 9.

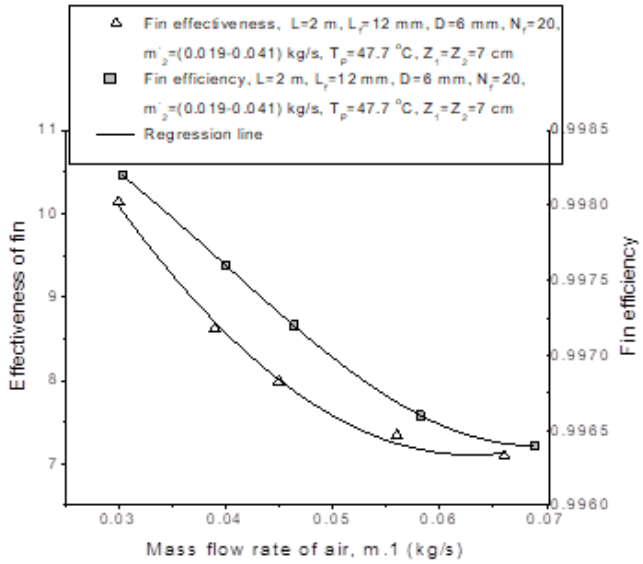

Fig. 8 Variation of efficiency and effectiveness of fin with mass flow rates of air in longitudinal fin inline hole jet plate solar air heater at fixed jet hole diameter (D = 6 mm)

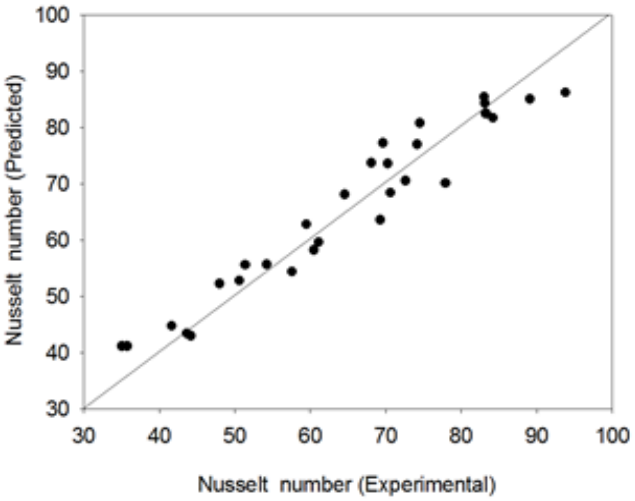

Fig. 9 Parity plot between predicted and experimental values of Nusselt number for longitudinal fins cross flow inline hole jet plate solar air heater at fixed jet hole diameter (D = 6 mm)

5.5.2 Correlation for friction factor

The negative exponents of the Reynolds number (Re_{ja2}) and pitch of the fins (p) show the friction factor decreases with increase of Reynolds number (Re_{ja2}) and pitch of the fins (p) in the jet plate solar air heater with longitudinal fins for fixed depth of the channel, Z_2 (7.0 cm), whereas the depth of the upper channel (Z_2) directly affects on the friction factor due to its positive exponent in the above correlated function for the friction factor at fixed pitch of the fins (p). The correlation coefficient of 0.97 indicates the goodness of fit in cross flow jet plate solar air heater with longitudinal fins as shown in Fig. 10.

$$f_s = 0.08\ (Re_{ja2})^{-0.3035}\ (Z_2 / p)^{1.5} \quad (12)$$

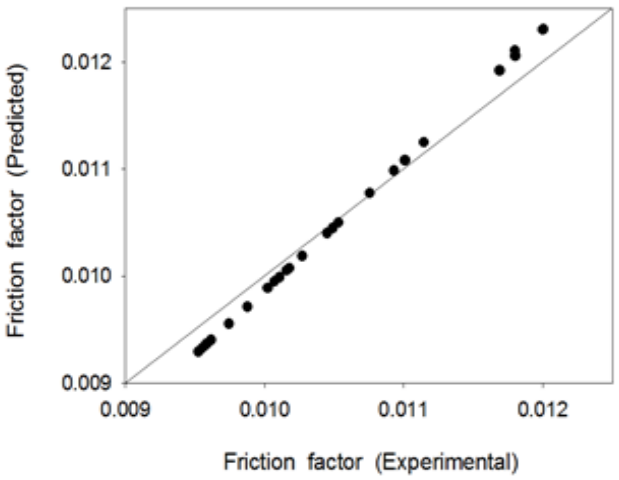

Fig. 10 Parity plot between predicted and experimental values of friction factor for longitudinal fins cross flow inline hole jet plate solar air heater at fixed jet hole diameter, (D = 6 mm)

5.5.3 Correlation for effectiveness of the fin (ξ)

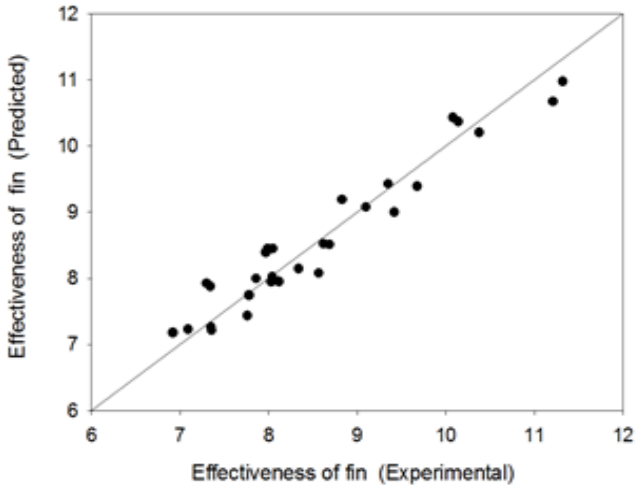

Fig. 11 Parity plot between predicted and experimental values of effectiveness of fin for longitudinal fins cross flow inline hole jet plate solar air heater at fixed jet hole diameter, D (6 mm)

The Reynolds number (Re_{ja2}) and pitch of the fins (p) inversely affect the effectiveness of the fin (ξ) due to its negative exponent in the correlated function, which indicates the effectiveness of fin (ξ) decreases with increase in mass flow rates of air ($\dot{m}_1$ and $\dot{m}_2$) and pitch of the fins (p) in jet plate solar air heater with longitudinal fins, whereas the positive exponents of depth of upper channel (Z_2) show the direct effect on the effectiveness of the fin (ξ). The effectiveness of fin (ξ) increases with increasing Z_2 at fixed pitch of the fins, p (5.0 cm). A high correlation coefficient of 0.93 as shown in Fig. 11 shows goodness of fit.

$$\xi = 24.09\,(Re_{ja2})^{-0.434}\,(Z_2 / p)^{7.681} \quad (13)$$

6. CONCLUSIONS

From the present study, the following conclusions are made:

1. The considerable enhancement in heat transfer is found by providing longitudinal fins in a jet plate solar air heater.

2. The maximum increment in outlet air temperature (T_o) and collector efficiency (η_c) are found as 8% and 15.2% in jet plate solar air heater with longitudinal fins than cross flow jet plate solar air heater, whereas the maximum increment in outlet air temperature (T_o) and collector efficiency (η_c) are obtained as 4.1% and 56.0% in jet plate solar air heater with longitudinal fins as compared to non-cross flow jet plate solar air heater for fixed mass flow rate of air $\dot{m}_1$.

3. The maximum increment in Nusselt number (Nu_{Pj}) are obtained as 53.6% and 57.1% in jet plate solar air heater with longitudinal fins than cross and non-cross flow jet plate solar air heater for fixed Reynolds number (Re_{ja2}).

4. No significant change in friction factor has been observed in the air heater due to attaching the fins underside the absorber surface.

5. The new correlations for Nusselt number, friction factor and effectiveness of the fin have been developed and good relation has been found between the predicted and experimental values.

NOMENCLATURE

A	surface area of absorber plate, m^2
A_b	base area of the fin, m^2
A_c	cross-sectional area of the fin, m^2
A_j	area of jet hole, m^2
A_2	cross-sectional area of upper channel, m^2
C_p	specific heat capacity of air, kJ/kgK
d	air thickness between absorber and cover plate, m
D_2	hydraulic diameter of upper channel in cross flow air heater, m $D_2 = 4\,W\,Z_2 / 2\,(W + Z_2)$
D	diameter of jet hole, m
D_e	equivalent hydraulic diameter of upper channel in jet plate with longitudinal fins solar air heater, m $D_e = 4[pZ_2 - L_f\,\delta_f] / 2[(p + L_f]$
F_1	dimensionless constant
F_2	cross flow degradation factor
f_s	friction factor
h_{Pj}	average plate-to-jet air heat transfer coefficient, W/m^{2}K
I_T	incident solar flux, W/m^2
k_a	thermal conductivity of air flowing through duct, W/mK
k_{Al}	thermal conductivity of the fin material, W/mK
l_i	insulation thickness, m
L	collector length or width of fins, m
L_c	corrected length of the fins, m
L_f	length of the fins, m
m	dimensionless number
m'	fin parameter, m^{-1}
$\dot{m}_1$	mass flow rate of air through the lower channel, kg/sec
N	total number of holes in the jet plate
N_f	total number of fins underside the absorber plate
Nu_{Pj}	Nusselt number at upper channel
P_f	perimeter of the fin, m
p	pitch of the fins, m
Q_f	actual rate of heat transfer with fins, W
Q_{mf}	maximum rate of heat transfer from the fins, W
Q_{Nf}	rate of heat transfer without fin, W
Re_{ja2}	flow Reynolds number between absorber plate and jet plate
Re_D	jet Reynolds number
T_1	inlet air temperature at lower channel, ^{o}C
T_2	inlet air temperature at upper channel, ^{o}C
ΔT_1	difference of inlet air above jet plate in mixing of air and outlet air temperature, ^{o}C $\Delta T_1 = (T_o - T_i)$
ΔT_2	difference of absorber plate and air temperature at the upper channel, ^{o}C $\Delta T_2 = (T_P - T_{a2})$
T_A	ambient air temperature, ^{o}C
T_{a1}	air temperature at lower channel, ^{o}C
T_{a2}	air temperature at upper channel, ^{o}C
T_i	inlet air temperature above jet plate in mixing of air, ^{o}C
T_o	outlet air temperature, ^{o}C
T_{ol}	outlet air temperature at jet hole, ^{o}C
T_P	absorber plate temperature, ^{o}C

$\overline{V}_1$ wetted mean inlet air velocity in the lower channel, m/sec
$\overline{V}_2$ wetted mean inlet air velocity in the upper channel, m/sec
$\overline{V}_o$ wetted mean outlet air velocity in the upper channel, m/sec
V_j jet air velocity, m/sec
$\overline{V}_{av}$ average velocity of air in the upper channel, m/sec
$\overline{V}$ average velocity of V_{av} and V_o in upper channel, m/sec
X span-wise pitch of the jet holes, m
Y stream-wise pitch of jet holes, m
W width of the solar air heater, m
Z_1 distance between the jet plate and the bottom plate, m
Z_2 distance between the absorber plate and the jet plate, m
ρ density of air, kg/m^3
δ_f thickness of the fins, m
μ dynamic viscosity of air, Pa.sec
ω uncertainty

Greek Symbols
η collector efficiency
η_f fin efficiency
θ tilt angle
ξ effectiveness of the fin

Subscript
Al aluminum
i inlet air at upper channel
j jet air / jet plate
o outlet air at heater exit
ol outlet air at jet hole
P absorber plate
t thickness

REFERENCES

Aboghrara, A.M., Baharudin, B.T.H.T., Alghoul, M.A., Adam, N.M., Hairuddin, A.A., and Hasan, H.A., 2017, "Performance analysis of solar air heater with jet impingement on corrugated absorber plate," *Case Studies in Thermal Engineering*, **10**, 111-120.
https://dx.doi.org/10.1016/j.csite.2017.04.002

Aboghrara, A.M., Alghoul, M.A., Baharudin, B.T.H.T., Elbreki, A.M., Ammar, A.A., Sopian, K., and Hairuddin, A.A., 2018, "Parametric study on the thermal performance and optimal design elements of solar air heater enhanced with jet impingement on a corrugated absorber plate," *International Journal of Photoenergy*, **2018**, 1-22.
https://dx.doi.org/10.1155/2018/1469385

Aharwal, K.R., Gandhi, B.K., and Saini, J.S., 2009, "Heat transfer and friction characteristics of solar air heater ducts having integral inclined discrete ribs on absorber plate," *International Journal of Heat and Mass Transfer*, **52**, 5970-5977.
https://dx.doi.org/10.1016/j.ijheatmasstransfer.2009.05.032

Akpinar, E.K., and Kocyigit, F., 2010, "Experimental investigation of thermal performance of solar air heater having different obstacles on absorber plates," *International Communications in Heat and Mass Transfer*, **37**(4), 416-421.
https://dx.doi.org/10.1016/j.icheatmasstransfer.2009.11.007

Belusko, M., Saman, W., and Bruno, F., 2008, "Performance of jet impingement in unglazed air collector," *Solar Energy,* **82**(5), 389-398.
https://dx.doi.org/10.1016/j.solener.2007.10.005

Chabane, F., Moummi, N., Benramache, S., Bensahal, D., and Belahssen, O., 2013a, "Collector efficiency by single pass of solar air heaters with and without using fins," *Engineering Journal*, **17**(3), 43-55.
https://dx.doi.org/10.4186/ej.2013.17.3.43

Chabane, F., Moummi, N., Brima, A., and Benramache, S., 2013b, "Thermal efficiency analysis of a single-flow solar air heater with different mass flow rates in a smooth plate," *Frontiers in Heat and Mass Transfer*, **4**, 013006, 1-6.
https://dx.doi.org/10.5098/hmt.v4.1.3006

Chabane, F., Moummi, N., and Benramache, S., 2014, "Experimental study of heat transfer and thermal performance with longitudinal fins of solar air heater," *Journal of Advanced Research*, **5**(2), 183-192.
https://dx.doi.org/10.1016/j.jare.2013.03.001

Chaudhury, C., and Garg, H.P., 1991, "Evaluation of a jet plate solar air heater," *Solar Energy*, **46**(4), 199-209.
https://dx.doi.org/10.1016/0038-092X(91)90064-4

Chauhan, R., and Thakur, N.S., 2013, "Heat transfer and friction factor correlation for impinging jet solar air heater," *Experimental Thermal and Fluid Science,* **44**, 760-767.
https://dx.doi.org/10.1016/j.expthermflusci.2012.09.019

Das, S., Biswas, A., and Das, B., 2022, "Numerical analysis of a solar air heater with jet impingement—comparison of performance between jet designs," *Journal of Solar Energy*, **144**(1), 011001.
https://dx.doi.org/10.1115/1.4051478

Farahani, S.D., and Shadi, M., 2021, "Optimization-decision making of roughened solar air heaters with impingement jets based on 3E analysis," *International Communications in Heat and Mass Transfer*, **129**, 105742.
https://dx.doi.org/10.1016/j.icheatmasstransfer.2021.105742

Flilihi, E., Sebbar, E.H., Achemlal, D., Rhafiki, T.E., Sriti, M., and Chaabelasri, E., 2022, "Effect of absorber design on convective heat transfer in a flat plate solar collector: A CFD modeling," *Frontiers in Heat and Mass Transfer*, **18**, 39, 1-6.
https://dx.doi.org/10.5098/hmt.18.39

Florschuetz, L.W., Metzger, D.E., and Truman, C.R., 1981, "Jet array impingement with cross flow-correlation of streamwise resolved flow and heat transfer distributions," *NASA Contractor Report*, **3373**.
https://ntrs.nasa.gov/api/citations/19810006721/downloads/19810006721.pdf
(Last accessed on 20th April, 2022).

Garg, H.P., Datta, G., and Bandyopadhyay, B., 1983, "A study on the effect of enhanced heat transfer area in solar air heaters," *Energy Conversion and Management*, **23**(1), 43-49.
https://dx.doi.org/10.1016/0196-8904(83)90007-9

Garg, H.P., Datta, G., and Bhargava, A.K., 1989, "Performance studies on a finned-air heater," *Energy*, **14**(2), 87-92.
https://dx.doi.org/10.1016/0360-5442(89)90082-0

Garg, H.P., Jha, R., Choudhury, C., and Datta, G., 1990, "Theoretical analysis on a new finned type solar air heater," In: Horigome, T., Kimura, K., Takakura, T., Nishino, T., and Fujii, I. (Editors), *International Solar Energy Society Proceedings Series*, Clean and Safe Energy Forever, Pergamon, 537-541.
https://dx.doi.org/10.1016/B978-0-08-037193-1.50110-5

Garg, H.P., Jha, R., Choudhury, C., and Datta, G., 1991, "Theoretical analysis on a new finned type solar air heater," *Energy*, **16**(10), 1231-1238.
https://dx.doi.org/10.1016/0360-5442(91)90152-C

Gupta, C.L., and Garg, H.P., 1967, "Performance studies on solar air heaters," *Solar Energy*, **11**(1), 25-31.
https://dx.doi.org/10.1016/0038-092X(67)90014-X

Global Digital Central
ISSN: 2151-8629

Gupta, D., Solanki, S.C., and Saini, J.S., 1993, "Heat and fluid flow in rectangular solar air heater ducts having transverse rib roughness on absorber plates," *Solar Energy*, **51**(1), 31-37.
https://dx.doi.org/10.1016/0038-092X(93)90039-Q

Hasan, H.A., Sopian, K., Jaaz, A.H., and Al-Shamani, A.N., 2017, "Experimental investigation of jet array nanofluids impingement in photovoltaic/thermal collector," *Solar Energy*, **144**, 321-334.
https://dx.doi.org/10.1016/j.solener.2017.01.036

Hassan, H., and AboElfadl, S., 2021, "Heat transfer and performance analysis of SAH having new transverse finned absorber of lateral gaps and central holes," *Solar Energy*, **227**, 236-258.
https://dx.doi.org/10.1016/j.solener.2021.08.061

Irfan, K., and Emre, T., 2006, "Experimental Investigation of solar air heater with free and fixed fins: Efficiency and exergy loss," *International Journal of Science and Technology*, **1**(1), 75-82.

Jaurker, A.R., Saini, J.S., and Gandhi, B.K., 2006, "Heat transfer and friction characteristics of solar air heater duct using rib-grooved artificial roughness," *Solar Energy*, **80**(8), 895-907.
https://dx.doi.org/10.1016/j.solener.2005.08.006

Karsli, S., 2007, "Performance analysis of new design solar air collectors for drying applications," *Renewable Energy*, **32**(10), 2007, 1645-1660.
https://dx.doi.org/10.1016/j.renene.2006.08.005

Kercher, D.M., and Tabakoff, W., 1970, "Heat transfer by a square array of round air jets impinging perpendicular to a flat surface including the effect of spent air," *Journal of Engineering for Gas Turbines and Power,* **92**(1), 73-82.
https://dx.doi.org/10.1115/1.3445306

Kline, S.J., and McKlintock, F.A., 1953, "Describing uncertainties in single sample experiments," *Mechanical Engineering*, **75**, 3-8.

Kumar, N., Kumar, A., and Maithani, R., 2020, "Development of new correlations for heat transfer and pressure loss due to internal conical ring obstacles in an impinging jet solar air heater passage," *Thermal Science and Engineering Progress*, **17**, 100493.
https://dx.doi.org/10.1016/j.tsep.2020.100493

Kumar, R., Nadda, R., Kumar, S., Kumar, K., Afzal, A., Razak, R.K.A., and Sharifpur, M., 2021a, "Heat transfer and friction factor correlations for an impinging air jets solar thermal collector with arc ribs on an absorber plate," *Sustainable Energy Technologies and Assessments*, **47**, 101523.
https://dx.doi.org/10.1016/j.seta.2021.101523

Kumar, S., Thakur, R., Suri, A.R.S., Kashyap, K., Singhy, A., Kumar, S., and Kumar, A., 2021b, "A comprehensive review of performance analysis of with and without fins solar thermal collector," *Frontiers in Heat and Mass Transfer*, **16**(4), 1-11.
https://dx.doi.org/10.5098/hmt.16.4

Kurtbas, I., and Turgut, E., 2006, "Experimental investigation of solar air heater with free and fixed fins: Efficiency and energy loss," *International Journal of Science and Technology*, **1**(1), 75-82.

Maithani, R., Sharma, S., and Kumar, A., 2021, "Thermo-hydraulic and exergy analysis of inclined impinging jets on absorber plate of solar air heater," *Renewable Energy*, **179**, 84-95.
https://dx.doi.org/10.1016/j.renene.2021.07.013

Matheswaran, M.M., Arjunan, T.V., and Somasundaram, D., 2018, "Analytical investigation of solar air heater with jet impingement usingenergy and exergy analysis," *Solar Energy*, **161**, 25-37.
https://dx.doi.org/10.1016/j.solener.2017.12.036

McAdams, W.H., 1954, *Heat Transmission*, 3rd ed., McGraw-Hill, New York.

Metzger, D.E., Florschuetz, L.W., Takeuchi, D.I., Behee, R.D., and Berry, R.A., 1979, "Heat transfer characteristics for inline and staggered arrays of circular jets with cross-flow of spent air," *Journal of Heat Transfer*, **101**(3), 526-531.
https://dx.doi.org/10.1115/1.3451022

Moffat, R.J., 1988, "Describing the uncertainties in experimental results," *Experimental Thermal and Fluid Science*, **1**(1), 3-17.
https://dx.doi.org/10.1016/0894-1777(88)90043-X

Moshery, R., Chai, T.Y., Sopian, K., Fudholi, A., and Al-Waeli, A.H.A., 2021, "Thermal performance of jet-impingement solar air heater with transverse ribs absorber plate," *Solar Energy*, **214**, 355-366.
https://dx.doi.org/10.1016/j.solener.2020.11.059

Nadda, R., Kumar, A., and Maithani, R., 2017, "Developing heat transfer and friction loss in an impingement jets solar air heater with multiple arc protrusion obstacles," *Solar Energy*, **158**, 117-131.
https://dx.doi.org/10.1016/j.solener.2017.09.042

Nayak, R.K., and Singh, S.N, 2016, "Effect of geometrical aspects on the performance of jet plate solar air heater," *Solar Energy*, **137**, 434-440.
https://dx.doi.org/10.1016/j.solener.2016.08.024

Nayak, R.K., Prasad, R.S., Nayak, U.K., and Gupta, A.K., 2022, "Analytical study of thermal performance of a jet plate solar air heater with the longitudinal fins under the cross flow and non-cross flow conditions," *Frontiers in Heat and Mass Transfer*, **19**, 7, 1-12.
https://dx.doi.org/10.5098/hmt.19.7

Pazarlioğlu, H.K., Ekiciler, R., and Arslan, K, 2021, "Numerical analysis of effect of impinging jet on cooling of solar air heater with longitudinal fins," *Heat Transfer Research*, **52**(11), 47-61.
https://dx.doi.org/10.1615/HeatTransRes.2021037251

Perry, K.P., 1954, "Heat transfer by convection from a hot gas jet to a plane surface," *Proc. Inst. Mech. Engg.,* **168**(30), 775-780.

Prasad, B.N., and Saini, J.S., 1988, "Effect of artificial roughness on heat transfer and friction factor in a solar air heater," *Solar Energy*, **41**(6), 555-560.
https://dx.doi.org/10.1016/0038-092X(88)90058-8

Rajaseenivasan, T., Prasanth, S.R., Antony, M.S., and Srithar, K., 2017, "Experimental investigation on the performance of an impinging jet solar air heater," *Alexandria Engineering Journal*, **56**(1), 63-69.
https://dx.doi.org/10.1016/j.aej.2016.09.004

Romdhane, B.S., 2007, "The air solar collectors: Comparative study, introduction of baffles to favor the heat transfer," *Solar Energy*, **81**(1), 2007, 139-149.
https://dx.doi.org/10.1016/j.solener.2006.05.002

Sahu, M.M., and Bhagoria, J.L., 2005, "Augmentation of heat transfer coefficient by using 90º broken transverse ribs on absorber plate of solar air heater," *Renewable Energy*, **30**(13), 2057-2073.
https://dx.doi.org/10.1016/j.renene.2004.10.016

Salman, M., Chauhan, R., and Kim, S.C., 2021a, "Exergy analysis of solar heat collector with air jet impingement on dimple-shape-roughened absorber surface," *Renewable Energy*, **179**, 918-928.
https://dx.doi.org/10.1016/j.renene.2021.07.116

Salman, M., Park, M.H., Chauhan, R., and Kim, S.C., 2021b, "Experimental analysis of single loop solar heat collector with jet impingement over indented dimples," *Renewable Energy*, **169**, 618-628.
https://dx.doi.org/10.1016/j.renene.2021.01.043

Salman, M., Chauhan, R., Poongavanam, G.K., Park, M.H., and Kim, S.C., 2022, "Utilizing jet impingement on protrusion / dimple heated plate to improve the performance of double pass solar heat collector," *Renewable Energy*, **181**, 653-665.
https://dx.doi.org/10.1016/j.renene.2021.09.082

Shetty, S.P., Madhwesh, N., and Karanth, K.V., 2021, "Numerical analysis of a solar air heater with circular perforated absorber plate," *Solar Energy*, **215**, 416-433.
https://dx.doi.org/10.1016/j.solener.2020.12.053

Singh, S., Chaurasiya, S.K., Negi, B.S., Chander, S., Nemś, M., and Negi, S., 2020, "Utilizing circular jet impingement to enhance thermal performance of solar air heater," *Renewable Energy*, **154**, 1327-1345.
https://dx.doi.org/10.1016/j.renene.2020.03.095

Singh, S.N., 2006, "Performance studies on continuous longitudinal fins solar air heater," *Journal of ISM, Dhanbad*, **2**.

Sivakumar, S., Siva, K., and Mohanraj, M., 2019, "Experimental thermodynamic analysis of a forced convection solar air heater using absorber plate with pin-fins," *Journal of Thermal Analysis and Calorimetry*, **136**, 39–47.
https://dx.doi.org/10.1007/s10973-018-07998-5

Soni, A., and Singh, S.N., 2017, "Experimental analysis of geometrical parameters on the performance of an inline jet plate solar air heater," *Solar Energy*, **148**, 149-156.
https://dx.doi.org/10.1016/j.solener.2017.03.081

Sukhatme, S. P., 1996, *Solar energy, Principles of Thermal Collection and Storage*, 2nd edition, Tata McGraw Hill Publishing Company Limited, New Delhi.

Thombre, S.B., and Sukhatme, S.P., 1995, "Turbulent flow heat transfer and friction factor characteristics of shrouded fin arrays with uninterrupted fins," *Experimental Thermal and fluid Science*, **10**(3), 388-396.
https://dx.doi.org/10.1016/0894-1777(94)00059-H

Verma, R., Chandra, R., and Garg, H.P., 1991, "Parametric studies on the corrugated solar air heaters with and without cover," *Renewable Energy*, **1**(3-4), 361-371.
https://dx.doi.org/10.1016/0960-1481(91)90045-Q

Vinod, P.D., and Singh, S.N., 2017, "Thermo-hydraulic performance analysis of jet plate solar air heater under cross flow condition," *International Journal of Heat and Technology*, **35**(3), 603-610.
https://dx.doi.org/10.18280/ijht.350317

Xing, Y., Spring, S., and Weigand, B., 2010, "Experimental and numerical investigation of heat transfer characteristics of inline and staggered arrays of impinging jets," *Journal of Heat Transfer*, **132**(9), 092201.
https://dx.doi.org/10.1115/1.4001633

Yadav, S., and Saini, R.P., 2020, "Numerical investigation on the performance of a solar air heater using jet impingement with absorber plate,"*Solar Energy*, **208**, 236-248.
https://dx.doi.org/10.1016/j.solener.2020.07.088

Yadav, S., and Saini, R.P., 2022, "Thermo-hydraulic CFD analysis of impinging jet solar air heater with different jet geometries," In: Kumar, R., Pandey, A.K., Sharma, R.K., and Norkey, G. (Editors), *Recent Trends in Thermal Engineering*, Lecture Notes in Mechanical Engineering. Springer, Singapore, 193-201.
https://dx.doi.org/10.1007/978-981-16-3132-0_19